**Supplementary Material**

# Effect of environmental factors on photovoltaic soiling: experimental and statistical analysis

**Honey Brahma [1,*], Shraiya Pant [1], Leonardo Micheli [2,*], Greg P. Smestad [3] and Nabin Sarmah [1]**

[1] Department of Energy, Tezpur University, Assam, 784028, India; honeybrahma325@gmail.com, shraiyapant@gmail.com, nabin@tezu.ernet.in
[2] Department of Astronautical, Electrical and Energy Engineering, Sapienza University of Rome, Rome, Italy; leonardo.micheli@uniroma1.it
[3] Sol Ideas Technology Development, P.O. Box 5729, San José, CA, 95150, USA; inquiries@solideas.com
* Correspondence: honeybrahma325@gmail.com, leonardo.micheli@uniroma1.it

***Dust characteristics for the location***

In order to provide a better overview of the location, the soiling experienced at this site was studied through Electron Dispersion X-ray Spectroscopy (EDS) and Field Emission Scanning Electron Microscopy (FESEM). The elemental composition of the particles deposited by soiling was obtained via FESEM-EDX by utilizing a Zeiss, Sigma unit. A FESEM image of the soiling sample provides the morphology and average particle size of the dust particles. FESEM analysis was done using a Ziess, GeminiSEM300. The soiling sample was collected from glass coupons mounted horizontally in the outdoor environment during July 2017 - April 2018 [1]. To determine the elemental composition, particles deposited via soiling were collected using a blade edge after they were deposited during the pre-monsoon season (in April 2018).

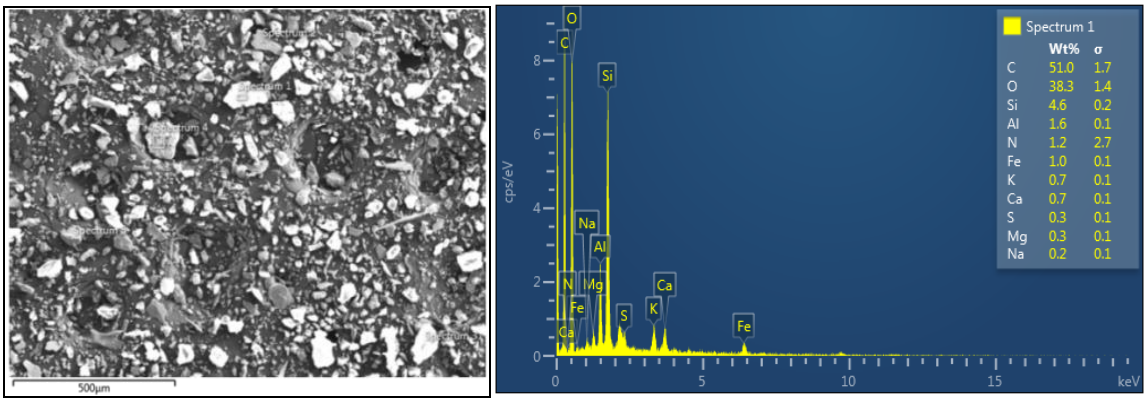


(a) (b)

**Figure S1.** EDS analysis: (a) Electron microscope (FESEM-EDX) image of the dust sample for EDS showing different particle sizes. The scale shown in the lower left is 500 µm. The image on the right (b) shows an example of an EDS spectrum of the dust sample showing peaks for various elements. The soiling was scraped off the glass coupon with a blade edge.

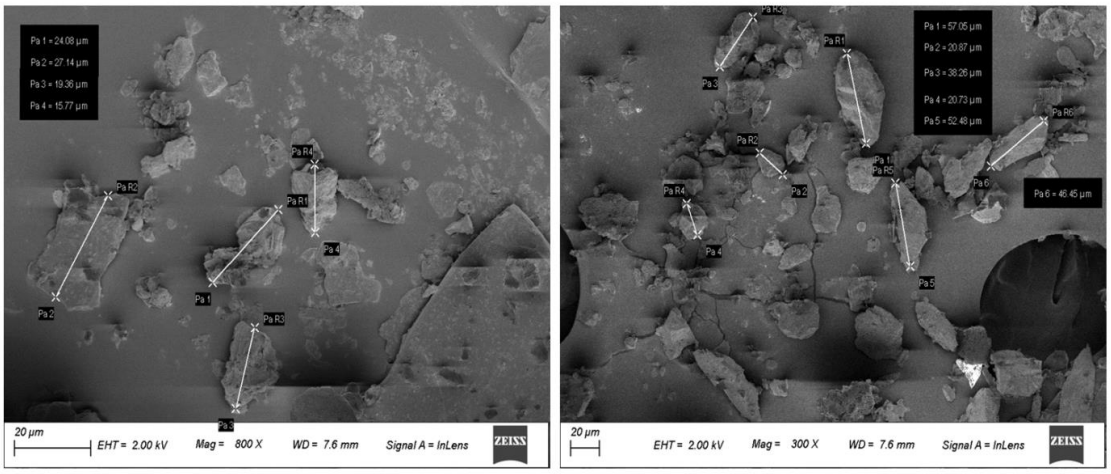


**Figure S2.** FESEM images of dust particles at a magnification 800x (left), and a magnification 300x (right). The soiling was scraped off the glass coupon with a blade edge. The lines shown in the image were used to determine the particle sizes.

**Table S1.** Elemental composition (in weight percentage) of dust from the outdoor experiment assessed by EDS. The sample is shown in Figure S1.

| Spectrum | C | O | Si | Al | N | Fe | K | Ca | S | Mg | Na |
|---|---|---|---|---|---|---|---|---|---|---|---|
| **Spectrum 1** | 51.0 | 38.3 | 4.6 | 1.6 | 1.2 | 1.0 | 0.7 | 0.7 | 0.3 | 0.3 | 0.2 |
| **Spectrum 2** | 54.6 | 34.8 | 5.8 | 1.6 | 0.0 | 1.5 | 0.6 | 0.4 | 0.0 | 0.4 | 0.3 |
| **Spectrum3** | 48.5 | 34.9 | 5.7 | 1.6 | 0.0 | 7.2 | 0.7 | 0.5 | 0.1 | 0.3 | 0.4 |
| **Spectrum 4** | 54.2 | 34.3 | 5.7 | 1.7 | 0.5 | 1.5 | 0.8 | 0.4 | 0.1 | 0.4 | 0.3 |
| **Spectrum 5** | 56.5 | 32.3 | 4.7 | 1.3 | 2.4 | 0.0 | 1.6 | 0.2 | 0.3 | 0.1 | 0.5 |
| **Mean** | 52.96 | 34.92 | 5.3 | 1.56 | 0.82 | 2.24 | 0.88 | 0.44 | 0.16 | 0.30 | 0.34 |
| **Standard Deviation** | 3.18 | 2.16 | 0.6 | 0.15 | 1.01 | 2.84 | 0.41 | 0.18 | 0.13 | 0.12 | 0.11 |

Previous researchers [2, 3] found within a radius of 250 km of Tezpur, clay, sillimanite ($Al_2SiO_5$), silica-based sand, granite ($SiO_2$, $Al_2O_3$, $K_2O$, $Na_2O$, CaO, trace Fe oxides, MgO, $TiO_2$) and limestone ($CaCO_3$). A soil sample collected by Khare et al. [4] within a radius of 160 km from the location revealed the presence of $NO_3^-$ and $SO_4^{2-}$ in the soil, emitted from the tea processing industries, brick kilns, and industrial coke ovens.

The mean and the standard deviation of the elemental weight percentages found in the soiling sample of the study are shown in Table S1. The major elements (Figure S1) were carbon, C (53%), and oxygen, O (35%), with minor amounts of other elements including silicon, Si (5.3%), iron, Fe (2.24%), aluminium, Al (1.56%), potassium, K (0.88%), nitrogen, N (0.82%), calcium, Ca (0.44%), sodium, Na (0.34%), magnesium, Mg (0.3%), and sulphur, S (0.16%). The source for the high percentage of carbon may be the vehicles inside the University campus (near the experimental site), and biomass used for cooking and heating purposes in the nearby households. The location under study often experiences high environmental PM10 levels due to the burning of kerosene and coal, and emissions from petroleum refining. Elements such as K, N, Ca, Na, Mg, and S may be in the form of ions [5]. The presence of oxygen as the major elemental composition of the dust at the location is attributed to various oxides of the elements. The presence of O, Si, Al, Fe, and Ca (the main earth crustal elements) may be due to the action of the wind. The S and Fe may be the result of coal combustion and industrial activities. The presence of K may be due to biomass and wood-burning. A similar composition of elements in the dust of this locality was reported by other researchers [4, 5].

The FESEM images connected to the EDS analysis for the dust sample collected from the glass coupons are provided in Figure S2. The particles removed from the glass coupons have different morphologies and particle sizes,

varying from 15.77 µm to 57.05 µm. The mean particle size was found to be 39.45 µm. Optical microscopy of the particles, while they were attached to the glass coupons (in situ), was presented in previous work, as well as a particle size distribution analysis [1]. The particle size in part determines the adhesiveness of the dust particles. The larger dust particles have less adhesion than the smaller dust particles [6]. In addition, the larger particles are more likely to be removed by the wind compared to the smaller particles [7].

***Environmental parameters (details)***

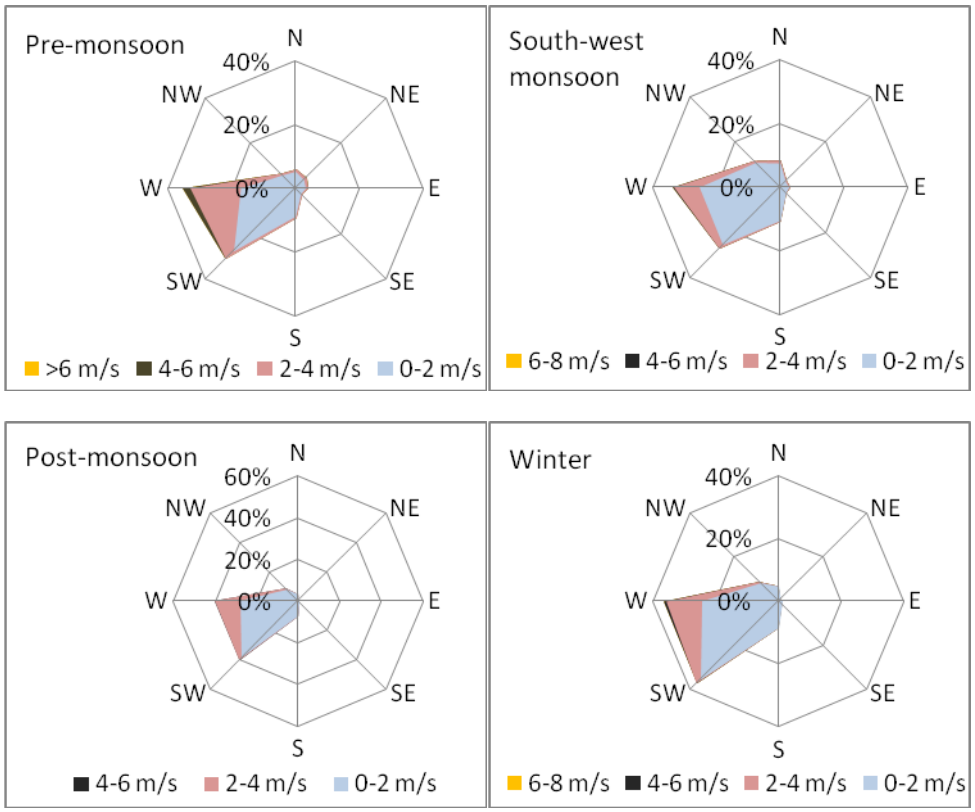


**Figure S3.** Rose diagram for the wind direction of four distinct seasons at the test site in Tezpur, India. The percentage distribution of different wind speed ranges for a season is represented by different color codes (yellow for 6-8 m/s, black for 4-6 m/s, red for 2-4 m/s, and blue for 0-2 m/s wind speed ranges).

**Table S2.** Distribution (percentage of total days) of wind speed for each of the four seasons.

| Wind speed (m/s) | SW monsoon (%) | Post-monsoon (%) | Winter (%) | Pre-monsoon (%) |
|---|---|---|---|---|
| **0-2** | 87.8 | 85.2 | 84.8 | 74.4 |
| **2-4** | 11.7 | 14.4 | 14.1 | 22.8 |
| **4-6** | 0.5 | 0.4 | 1.1 | 2.7 |
| **6-8** | <0.1 | - | <0.1 | 0.1 |
| **8-10** | - | - | - | <0.1 |
| **10-12** | - | - | - | <0.1 |

***Transmittance***

This work investigates the correlation between environmental parameters and loss in optical transmittance, as a proxy for the electrical losses due to soiling. The glass coupons used in the analysis are from earlier work [1] and

were all cleaned using water and a microfiber cloth before they were installed at the site. The experimental protocol was similar to that utilized in the prior work. Briefly, the direct spectral transmittance was recorded using a Thermo Scientific UV10 spectrophotometer. Separate measurements versus air were made for both the soiled sample and a clean glass coupon (see Figure S4c for the latter). The ratio of the two, for each wavelength, is the relative direct transmittance. Some representative plots are shown in Figure S4. The average relative direct transmittance, $\tau_r$, recorded weekly is the simple average of the spectral transmittance over the wavelength range 0.35-1 μm, averaged using three spots on each glass coupon.

As a quality control, the relative spectral transmittance curves were checked against the modified Ångström turbidity equation, previously shown to model the spectral behavior of many types of soiled glass samples worldwide. The modified Ångström turbidity equation is given by [1]:

$$\tau(\lambda) = \exp(-b\,\lambda^{-a}) + c \qquad \text{(S.1)}$$

where a and b are the parameters connected to the size and the surface coverage of the particles, respectively. The parameter c is an offset parameter (See Figure S4.). The selected boundary conditions for the parameters a, b, and c and the fit to Equation (S.1) were: $0.01 < a < 5$, $0 < b < 0.5$ and $< -0.35 < c < 0.1$

It was found that for a variety of possible reasons, the fit of the measured relative transmittance to Equation (S.1) can sometimes be poor, especially for lightly soiled glass coupons. Figure S4b shows such a curve with a low $R^2$ value and an unexpected spectral shape.

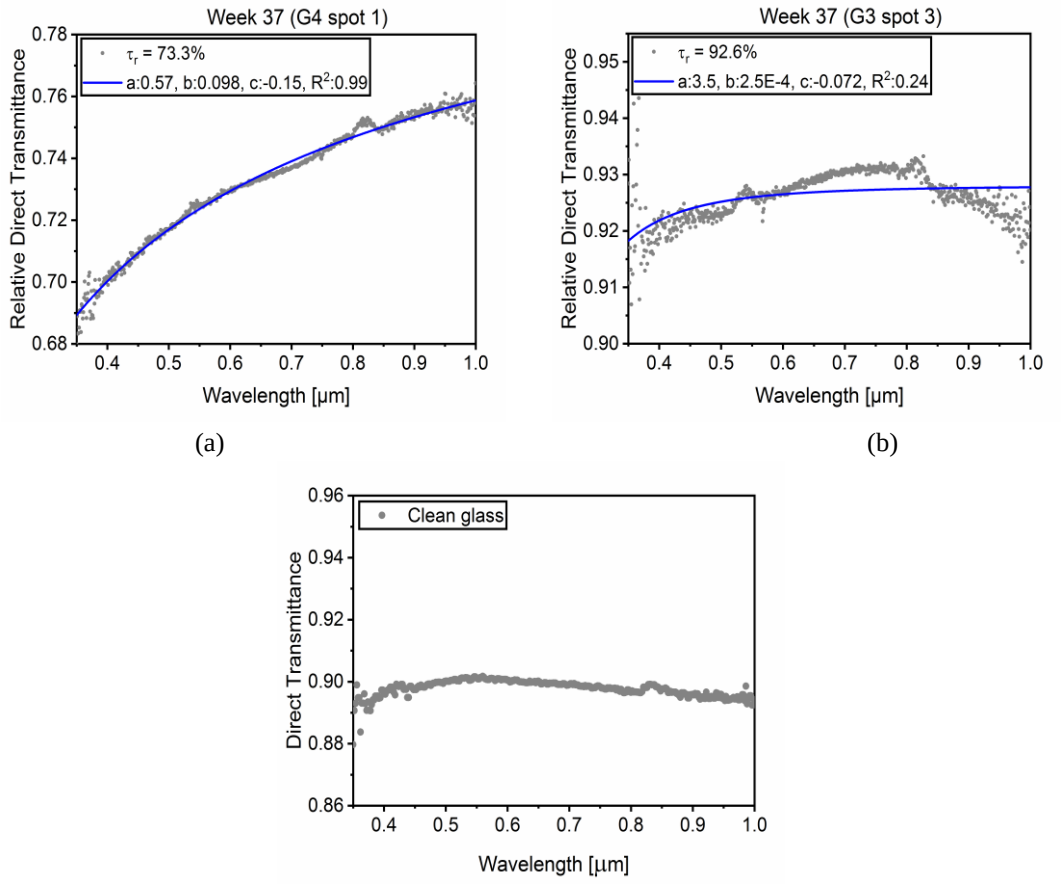


**Figure S4.** Examples of the direct relative transmittance data fit to the modified Ångström turbidity equation for glass coupons that exhibit (a) high $R^2$, (b) low $R^2$ values, and (c) direct transmittance of the clean glass coupon with air as a reference. The data points are shown for the week and the spot on the coupon as indicated.

Therefore, measurements were also made using a direct method, in which the relative transmittance is obtained by placing the clean glass in the reference compartment and the soiled glass in the sample compartment. These experiments indicated that the measurement error, or the difference between the indirect and direct measurement methods to obtain the average direct transmittance, was less than 0.4%.

To check the shape of the curve for multiple measurements, a plot of $\tau_r$ versus c was made in a similar way as was reported in the previous study [1]. The selection criteria considered for the modified Ångström equation fit are as follows: if the $R^2$ for the fit is less than 0.70 and the spectral transmittance data has more than 5 points in the range 0.35 to 0.4 µm greater than 1/2 of the spectral transmittance value at 1 µm, then the result can be discarded as an outlier (for example, see Figure S4b). The results of this analysis are displayed in Figure S5.

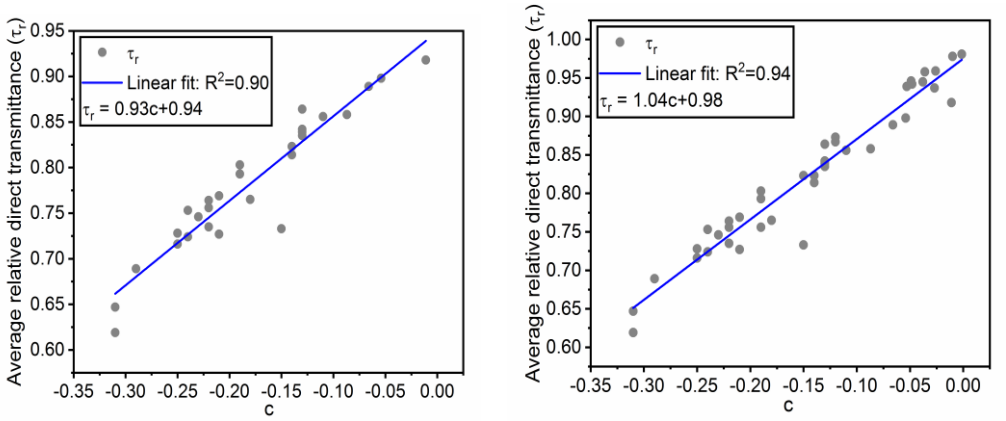


**Figure S5.** The average relative direct transmittance ($\tau_r$) versus offset parameter, c, of the modified Ångström turbidity equation for some selected weeks of the whole year (left), and just the winter season (right).

These exercises indicate that, for the most part, the transmittance data were of good quality and sufficient for the analysis that was conducted with it. A future report, for a study currently underway, will explore best measurement practices in soiling estimations using glass coupons.

***Statistical Analysis***

The standard deviation (SD) and uncertainty are calculated using Equation (S.2) and (S.3), respectively [8]:

$$SD = \sqrt{\frac{\sum_{i=1}^{n}(X_i - \mu)^2}{(n-1)}} \tag{S.2}$$

$$Uncertainty = \sqrt{\frac{\sum_{i=1}^{n}(X_i - \mu)^2}{n\,(n-1)}} \tag{S.3}$$

where $X_i$ is the $i^{th}$ reading in the dataset, µ is the mean of the dataset and n is the number of readings in the dataset. These equations were utilized, for example, for the average relative direct transmittance, $\tau_r$.

The MSE is defined as the mean of the squared difference between the measured and predicted data, it describes the variance of the residuals. The MSE is expressed as:

$$MSE = \frac{1}{N}\sum_{i=1}^{N}\left(x_{meaured,i} - x_{predicted,i}\right)^2 \quad \text{(S.4)}$$

where $i$ is the variable, $x_{measured,i}$ and $x_{predicted,i}$ are the measured predicted at the i[th] data point. $N$ is the number of data points.

The RMSE is the square root of the MSE; it quantifies the standard deviation of the residuals. The RMSE can be equated using:

$$RMSE = \sqrt{\frac{1}{N}\sum_{i=1}^{N}\left(x_{measured,i} - x_{predicted,i}\right)^2} \quad \text{(S.5)}$$

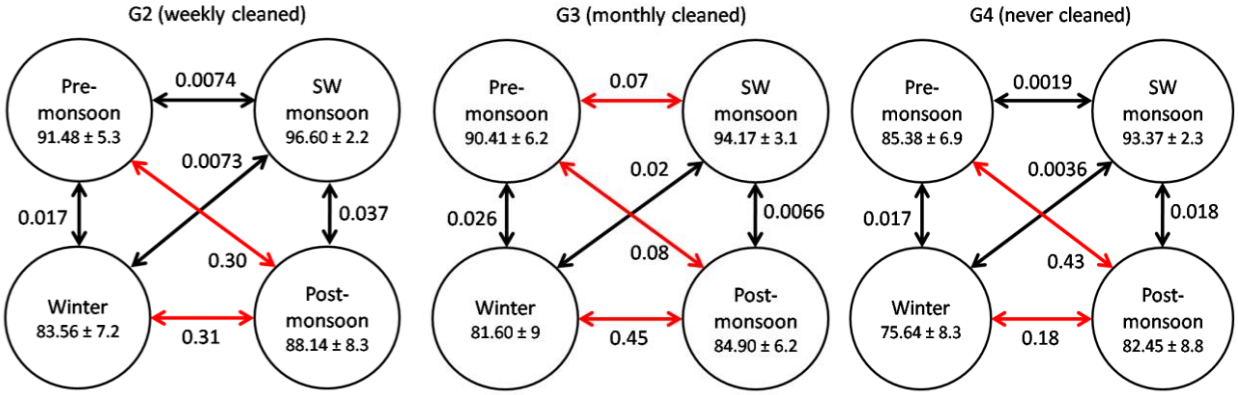


**Figure S6.** The t-test p-value of the combination of different seasons for the weekly cleaned (G2), monthly cleaned (G3), and never cleaned (G4) glass coupons. The relation between two seasons connected with a red arrow does not have a statistically significant difference in their mean values (p-value > 0.05), whereas those connected with a black arrow have a statistically significant difference in their mean values (p-value < 0.05). The means for the transmittance are indicated along with their SD values.

**Table S3.** The value of the indicated parameters and the $R^2$ value obtained from the logistic curve fitting [9] for the average relative direct transmittance of the glass coupons vs. the weekly maximum rainfall $R_{max}$, for different cleaning cycles: weekly cleaned (G2), monthly cleaned (G3) and never cleaned (G4), as shown in Figure 8 of the main text.

| Equation: $\tau_r$ =A2+(A1-A2)/(1+($R_{max}$/x0)^q) | | | | | | | |
|---|---|---|---|---|---|---|---|
| Glass Coupon | A1 | A2 | x0 | q | Reduced Chi-square | R-squared | Adjusted R-squared |
| G2 | 0.85 | 0.98 | 2.78 | 1.06 | 0.0027 | 0.46 | 0.42 |
| G3 | 0.83 | 0.95 | 2.40 | 1.34 | 0.0030 | 0.45 | 0.41 |
| G4 | 0.78 | 0.94 | 1.05 | 0.62 | 0.0044 | 0.43 | 0.39 |

The $R^2$ shows how well terms (data points) fit a curve or line. The adjusted $R^2$ also indicates how well terms fit a curve or line, but adjusts for the number of terms in a model.

***Average weekly transmittance versus water and PM***

Environmental parameters that influence soiling include RH and dew formation [10, 11]. The right conditions can result in condensation on the glass, and its occurrence can be related to the air temperature and the dew point temperature. We explored the correlation of these to the transmittance, $\tau_r$. The correlation obtained between the RH, PM10, and $\tau_r$ is shown in Figure S7. The average weekly $\Delta T$ is the difference between the average weekly air temperature ($T_{amb}$) and average weekly dew point temperature ($T_d$) (see Figure S7a.). Empirically, it was observed that condensation occurred on glass surfaces for conditions of high RH and $T_d \geq (T_{amb} - 2.5\ °C)$. This is given by the number of hours in a week when the condition was met. Figure S7b. shows the results for the study site.

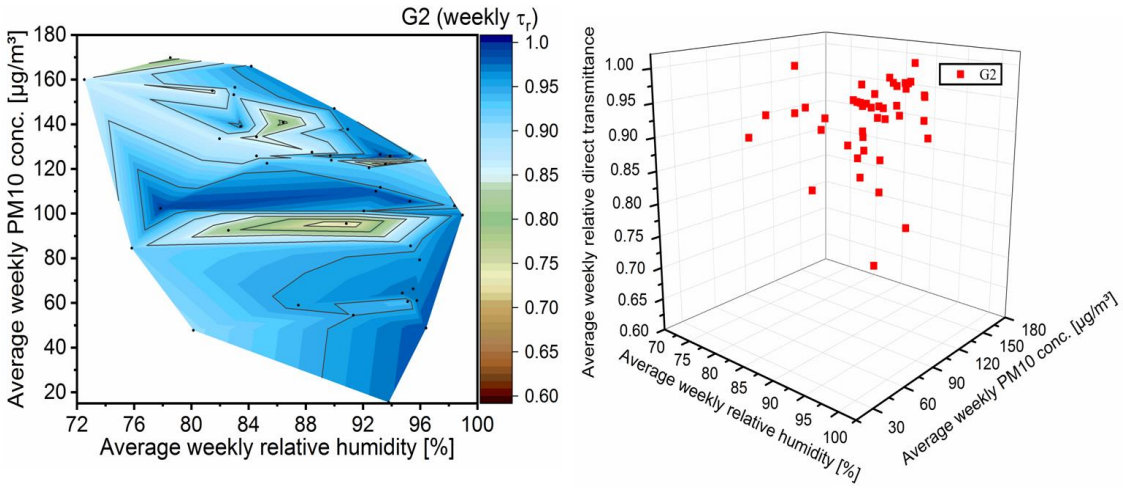


(a)

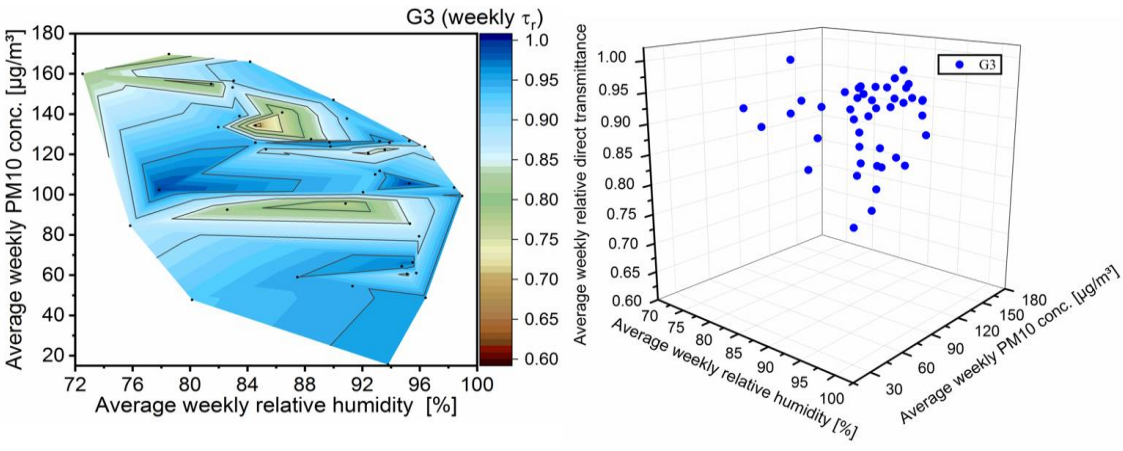


(b)

**Figure S7.** Correlation between the average relative direct transmittance ($\tau_r$), the average weekly PM10, and relative humidity (RH) for the glass coupon with different cleaning cycles: (a) weekly cleaned (G2) and (b) monthly cleaned (G3). The figure on the right shows the scatter plot for data on the left.

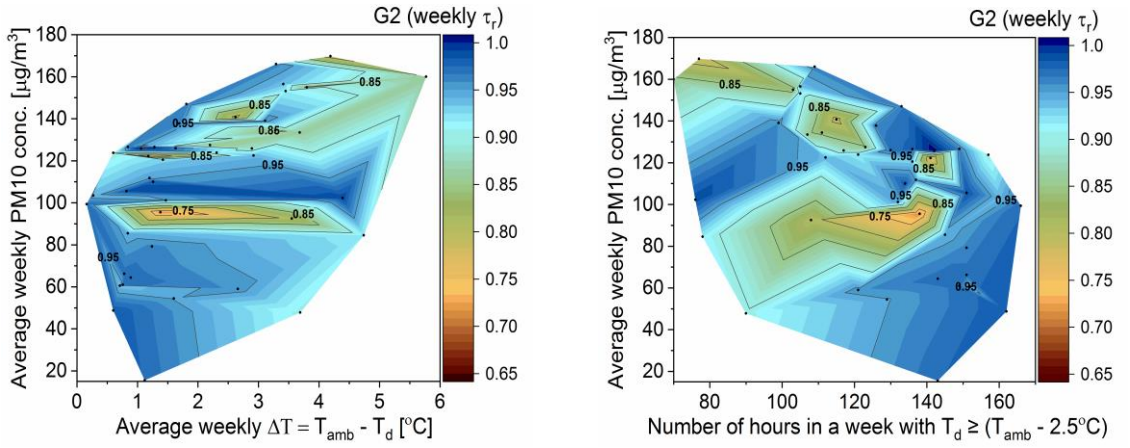


(a) (b)

**Figure S8.** Relation between average weekly relative direct transmittance ($\tau_r$), average weekly PM10 concentration, and (a) average weekly ΔT and (b) number of hours in a week with the condition $T_d \geq (T_{amb} - 2.5\ °C)$, for the weekly cleaned glass coupon G2.

It was observed that when PM10 < 80 μg/m$^3$, the $\tau_r$ is always greater than 90% irrespective of the ΔT. When PM10 > 80 μg/m$^3$, soiling is found to be prominent. A significant reduction in $\tau_r$ could be seen when PM10 is in the range of 80-120 μg/m$^3$ and ΔT is low. However, for PM10 > 120 μg/m$^3$ soiling occurs irrespective of the value of ΔT.

**Table S4.** The value of the parameters and the $R^2$ value obtained from the linear curve fitting for the average relative direct transmittance ($\tau_r$) vs. average air temperature ($T_{amb}$) for the weekly cleaned (G2), monthly cleaned (G3) and never cleaned (G4) glass coupons.

| Equation: $\tau_r$= Slope·$T_{amb}$+ Intercept | | | | | | |
|---|---|---|---|---|---|---|
| Glass coupons | Intercept | Slope | Residual sum of squares | Pearson's coefficient | R-squared | Adj. R-squared |
| G2 | 0.76 ± 0.026 | 0.011 ± 0.0017 | 0.098 | 0.72 | 0.52 | 0.50 |
| G3 | 0.73 ± 0.027 | 0.011 ± 0.0018 | 0.11 | 0.70 | 0.48 | 0.47 |
| G4 | 0.65 ± 0.029 | 0.016 ± 0.0019 | 0.12 | 0.78 | 0.61 | 0.60 |

**Table S5.** The value of the indicated parameters and the $R^2$ value obtained from the linear curve fitting for the average relative direct transmittance ($\tau_r$) vs. the average dew point temperature ($T_d$) for the weekly cleaned (G2), monthly cleaned (G3) and never cleaned (G4) glass coupons.

| Equation: $\tau_r$ = Slope·$T_d$+ Intercept | | | | | | |
|---|---|---|---|---|---|---|
| Glass coupons | Intercept | Slope | Residual sum of squares | Pearson's coefficient | R-squared | Adj. R-squared |
| G2 | 0.79 ± 0.019 | 0.010 ± 0.0015 | 0.093 | 0.74 | 0.54 | 0.53 |
| G3 | 0.77 ± 0.021 | 0.010 ± 0.0016 | 0.11 | 0.71 | 0.50 | 0.49 |
| G4 | 0.70 ± 0.020 | 0.014 ± 0.0015 | 0.10 | 0.82 | 0.67 | 0.66 |

Tables S4 and S5 show the parameters obtained from a linear correlation between the average relative direct transmittance of the weekly cleaned glass (G2) and average air temperature ($T_{amb}$) and average dew point temperature ($T_d$), respectively, for the different cleaning cycles for the whole year.

***Linear regression analysis***

Both the single-variable linear regression (SLR) and multi-variable linear regression (MLR) models have been used to correlate the environmental parameters to the average direct transmittance of the glass coupons. This was accomplished by employing the Regression Tool in the Data Analysis section in Excel 2016. The corrections obtained in this way are shown in the right-hand column of Table S6.

**Table S6.** The correlation values obtained using single-variable linear regression (SLR) models between the average relative direct transmittance of the weekly cleaned glass coupon (G2) and the average weekly value of various environmental parameters: rainfall intensity (Rain), frequency of rainfall ($R_f$), relative humidity (RH), particulate matter (PM10), ambient air temperature ($T_{amb}$) and dew point temperature ($T_d$). The analysis was performed using the data for a full year.

| Season | Environmental parameters | Model | R-squared | Adj. R-squared | Standard Error | p-value | Correlation |
|---|---|---|---|---|---|---|---|
| 1-year analysis | Rain | SLR | 0.26 | 0.24 | 0.060 | <0.05 | $\tau_r = 0.0068\ Rain + 0.89$ |
| | $R_f$ | | 0.27 | 0.26 | 0.059 | <0.05 | $\tau_r = 0.016\ R_f + 0.88$ |
| | $R_{max}$ | | 0.31 | 0.29 | 0.058 | <0.05 | $\tau_r = 0.0043\ R_{max} + 0.89$ |
| | RH | | 0.15 | 0.13 | 0.064 | <0.05 | $\tau_r = 0.0041\ RH + 0.56$ |
| | PM10 | | 0.095 | 0.073 | 0.066 | <0.05 | $\tau_r = -0.00058\ PM10 + 0.98$ |
| | $T_{amb}$ | | 0.52 | 0.51 | 0.048 | <0.05 | $\tau_r = 0.011T_{amb} + 0.76$ |
| | $T_d$ | | 0.56 | 0.55 | 0.046 | <0.05 | $\tau_r = 0.011T_d + 0.79$ |

**Table S7.** The correlation values between the measured and predicted average relative direct transmittance obtained from a multi-variable linear regression (MLR) model of the weekly cleaned glass coupon (G2) for various seasons and annually as shown in Figures 10, 11, and 12 of the main text.

| Season | Environmental parameters | Intercept | Slope | Residual sum of squares | Pearson's coefficient | R-squared | Adj. R-squared |
|---|---|---|---|---|---|---|---|
| Pre-monsoon | $R_f$ and Ws | 0.27 ± 0.13 | 0.70 ± 0.14 | 0.0065 | 0.84 | 0.70 | 0.67 |
| | Rain andPM10 | 0.29 ± 0.13 | 0.67 ± 0.15 | 0.0068 | 0.82 | 0.67 | 0.64 |
| Post-monsoon | Ws | 0.11 ± 0.13 | 0.88 ± 0.15 | 0.0044 | 0.94 | 0.88 | 0.86 |
| | $R_f$ | 0.16 ± 0.15 | 0.81 ± 0.17 | 0.0063 | 0.90 | 0.81 | 0.77 |
| Winter | Rain and Ws | 0.026 ± 0.073 | 0.97 ± 0.08 | 0.0010 | 0.98 | 0.97 | 0.96 |
| | $R_{max}$ and Ws | 0.034 ± 0.083 | 0.96 ± 0.10 | 0.0010 | 0.98 | 0.96 | 0.95 |

**Table S8.** Values for the linear fit parameters for the annual analysis using MLR. This was used for the regression plot of predicted and measured transmittance for the weekly cleaned glass (G2) using an MLR model for the whole year. The result is given in Figure 13 of the main text.

| Linear Fit: $\tau_r$ (Predicted) = Slope·$\tau_r$ (Measured) + Intercept | | | | | |
|---|---|---|---|---|---|
| Intercept | Slope | Residual sum of squares | Pearson's coefficient | R-squared | Adj. R-squared |
| 0.42 ± 0.071 | 0.53 ± 0.077 | 0.050 | 0.73 | 0.53 | 0.52 |

**Table S9.** Values for the exponential fit parameters for the annual analysis using MLR. This was used for the regression plot of predicted and measured transmittance for the weekly cleaned glass (G2) using an MLR model for the whole year. The result is given in Figure 13 of the main text.

| Exponential fit: $\tau_r$ (Predicted) = A· exp(B· $\tau_r$ (Measured)) + Offset | | | | | |
|---|---|---|---|---|---|
| A | B | Offset | Reduced Chi-square | R-squared | Adj. R-squared |
| 7.5E-6 ± 3.3E-5 | 9.91 ± 4.17 | 0.84 ± 0.028 | 0.0010 | 0.60 | 0.58 |

***Energy loss analysis***

The energy loss estimation due to soiling is beneficial to photovoltaic (PV) installers, as it can help predict the optimal cleaning frequency. The seasonal and annual energy losses due to soiling under standard test conditions (STC) have been calculated for glass coupons with different cleaning cycles. The electrical specification that has been used in the calculation of energy loss is presented in Table S10, and the equations used in the calculation are in Section 2.3 of the main text. The weekly energy yield loss for different cleaning cycles during the four seasons is shown in Figure S10. Future work will include the energy loss analysis under the actual spectral conditions.

**Table S10.** Electrical data of the PV module used to estimate the energy losses.

| Vikram Solar (SOMERA VSM.72.AAA.03.04 Monocrystalline) | |
|---|---|
| Power wattage $P_{max}[W_p]$ | 340 |
| Maximum voltage $V_{mpp}[V]$ | 37.98 |
| Maximum current $I_{mpp}[A]$ | 8.95 |
| Open-circuit voltage $V_{oc}[V]$ | 47.1 |
| Short-circuit current $I_{sc}[A]$ | 9.42 |
| Efficiency η [%] | 17.52 |
| Area [$m^2$] | 1.94 |

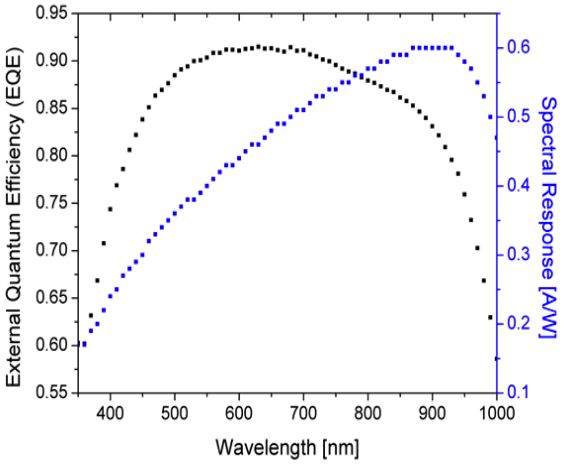


**Figure S9.** The external quantum efficiency and spectral response of a monocrystalline silicon solar cell of the BP Solar *Saturn Series* fabricated with Laser Grooved Buried Contact (LGBC) technology. The spectral response has been used in the calculation of the predicted soiling ratio ($r_s$) as given in Equation (10) of the main text.

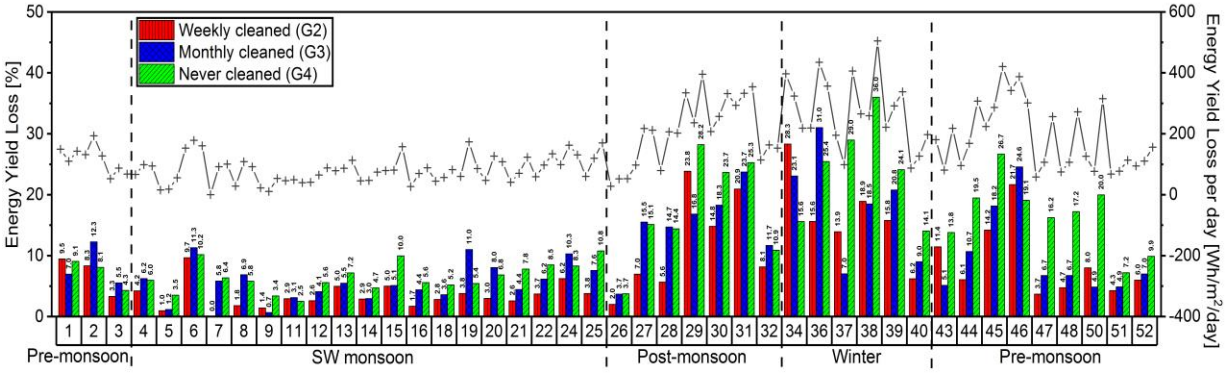


**Figure S10.** Energy yield loss, at standard test conditions (STC), due to soiling for different cleaning cycles during the four seasons. The plus symbol utilized for the right-side y-axis depicts the energy yield loss in Wh/m$^2$/day. This is a detailed (week-by-week) presentation of the results shown in Figure 15 in the main text.

## References


1. Smestad, G. P.; Germer, T. A.; Alrashidi, H.; Fernández, E. F.; Dey, S.; Brahma, H.; Sarmah, N.; Ghosh, A.; Sellami, N.; Hassan, I. A.; Desouky, M.; Kasry, A.; Pesala, B.; Sundaram, S.; Almonacid, F.; Reddy, K. S.; Mallick, T. K.; Micheli, L., Modelling photovoltaic soiling losses through optical characterization. *Scientific Reports* **2020,** 10, (1), 1-13.
2. Ministry of Mines, Minerals blocks on auction in 2018-19. In *4th National Conclave on Mines and Minerals 2018* Government of Assam, Ed. Indore, 2018.
3. Indian Bureau of Mines, Indian Minerals Yearbook 2015 (Part I) State Reviews( Assam). In 54th ed.; Ministry of Mines, G. o. I., Ed. Indian Bureau of Mines: Nagpur, 2017.
4. Khare, P.; Baruah, B. P., Elemental characterization and source identification of PM2.5 using multivariate analysis at the suburban site of North-East India. *Atmospheric Research* **2010,** 98, (1), 148-162.
5. Bhuyan, P.; Deka, P.; Prakash, A.; Balachandran, S.; Hoque, R. R., Chemical characterization and source apportionment of aerosol over mid Brahmaputra Valley, India. *Environmental Pollution* **2018,** 234, 997-1010.
6. Said, S. A.; Walwil, H. M., Fundamental studies on dust fouling effects on PV module performance. *Solar Energy* **2014,** 107, 328-337.
7. El-Shobokshy, M.; Mujahid, A.; Zakzouk, A., Effects of dust on the performance of concentrator photovoltaic cells. *IEE Proceedings I (Solid-State and Electron Devices)* **1985,** 132, (1), 5-8.
8. Meyer, V. R., Measurement uncertainty. *Journal of Chromatography A* **2007,** 1158, (1-2), 15-24.
9. Javed, W.; Guo, B.; Figgis, B.; Pomares, L. M.; Aïssa, B., Multi-year field assessment of seasonal variability of photovoltaic soiling and environmental factors in a desert environment. *Solar Energy* **2020,** 211, 1392-1402.
10. Figgis, B.; Nouviaire, A.; Wubulikasimu, Y.; Javed, W.; Guo, B.; Ait-Mokhtar, A.; Belarbi, R.; Ahzi, S.; Rémond, Y.; Ennaoui, A., Investigation of factors affecting condensation on soiled PV modules. *Solar Energy* **2018,** 159, 488-500.
11. Ilse, K.; Figgis, B.; Khan, M. Z.; Naumann, V.; Hagendorf, C., Dew as a detrimental influencing factor for soiling of PV modules. *IEEE Journal of Photovoltaics* **2018,** 9, (1), 287-294.